Metabolic Engineering Communications 7 (2018) e00075

Contents lists available at ScienceDirect

Metabolic Engineering Communications

journal homepage: www.elsevier.com/locate/mec

CO_2 to succinic acid – Estimating the potential of biocatalytic routes

Ulf W. Liebal, Lars M. Blank*, Birgitta E. Ebert

Institute of Applied Microbiology-iAMB, Aachen Biology and Biotechnology-ABBt, RWTH Aachen University, Worringer Weg 1, D-52074 Aachen, Germany

ARTICLE INFO

Keywords:
Carbon fixation
Metabolic engineering
Flux Balance Analysis
Succinic acid
Profitability
C1 carbon source

ABSTRACT

Microbial carbon dioxide assimilation and conversion to chemical platform molecules has the potential to be developed as economic, sustainable processes. The carbon dioxide assimilation can proceed by a variety of natural pathways and recently even synthetic CO_2 fixation routes have been designed. Early assessment of the performance of the different carbon fixation alternatives within biotechnological processes is desirable to evaluate their potential. Here we applied stoichiometric metabolic modeling based on physiological and process data to evaluate different process variants for the conversion of C1 carbon compounds to the industrial relevant platform chemical succinic acid. We computationally analyzed the performance of cyanobacteria, acetogens, methylotrophs, and synthetic CO_2 fixation pathways in *Saccharomyces cerevisiae* in terms of production rates, product yields, and the optimization potential. This analysis provided insight into the economic feasibility and allowed to estimate the future industrial applicability by estimating overall production costs. With reported, or estimated data of engineered or wild type strains, none of the simulated microbial succinate production processes showed a performance allowing competitive production. The main limiting factors were identified as gas and photon transfer and metabolic activities whereas metabolic network structure was not restricting. In simulations with optimized parameters most process alternatives reached economically interesting values, hence, represent promising alternatives to sugar-based fermentations.

1. Introduction

Succinic acid is a valuable platform chemical for the production of bio-based polymers such as nylons and polyesters but is also valuable itself as surfactant, chelator, and as an additive in the agricultural, food, and pharmaceutical industry (Ahn et al., 2016; Bozell and Petersen, 2010; Mazière et al., 2017). Succinic acid is conventionally synthesized petrochemically with an overall market size of about 60 kt in 2015 (Jansen and van Gulik, 2014; marketsandmarkets.com, 2016) and highly optimistic projections of more than 600 kt exist for 2020 (Choi et al., 2015; Pinazo et al., 2015). Conventional, large-scale, centralized chemical production plants inhibit modernization of process design and create hurdles for start-ups and new incomers (Clomburg et al., 2017). Instead, start-ups turn to biotechnological fermentation-based strategies with lower requirements for capital investment thus allowing for more dynamic market adaptations and better adjustment to niche requirements (Clomburg et al., 2017). As a consequence, bio-based production of succinic acid is advancing in recent years, and to date, a variety of microorganisms has been engineered for the synthesis of succinic acid from sugars, glycerol or acetate (Ahn et al., 2016; Becker et al., 2015; Pinazo et al., 2015; Valderrama-Gomez et al., 2016). Current production hosts include *Basfia succiniciproducens*, *Escherichia coli*, *Pichia kudriavzevii*, and *Saccharomyces cerevisiae*, which synthesize succinic acid via different metabolic production routes such as the oxidative or reductive TCA cycle or the glyoxylate shunt (Ahn et al., 2016; Becker et al., 2015; Choi et al., 2015). The processes have been optimized to reach titers of more than 100 g/l of succinic acid (Cui et al., 2017; Zhu et al., 2014) and productivities of more than 3 g/l/h (Ahn et al., 2016; Becker et al., 2015). Hence, fermentative succinic acid production is already cost-competitive with respect to petrochemical-based strategies (Mazière et al., 2017) and significant future saving potentials have been predicted (Pinazo et al., 2015; Santos et al., 2016).

In order to establish a truly circular bio-economy and to valorize the abundant, industrial byproduct CO_2, the replacement of sugar-based substrates with CO_2 is today of particular relevance (Ampelli et al., 2015; Dürre and Eikmanns, 2015; Mohan et al., 2016; Nybo et al., 2015). In the following alternative CO_2 fixation routes and examples are reviewed.

1.1. Anaerobic carbon fixation

Gas fermentations using syngas or H_2/CO_2 mixtures are being developed to utilize alternative substrates to petroleum and synthesize

* Correspondence to: Institute of Applied Microbiology-iAMB, Aachen Biology and Biotechnology-ABBt, RWTH Aachen University, Worringer Weg 1, D-52074 Aachen, Germany.
E-mail address: lars.blank@rwth-aachen.de (L.M. Blank).

https://doi.org/10.1016/j.mec.2018.e00075
Received 13 March 2018; Received in revised form 7 June 2018; Accepted 25 June 2018

value-added products. Acetogens in the bacterial Clostridia class are frequently used for carbon fixation using CO_2/H_2 or syngas mixtures under anaerobic conditions (Daniell et al., 2012; Phillips et al., 2017). Due to energetic challenges, these gas fermentations are limited to the production of short-chain chemicals (Fast and Papoutsakis, 2012). To overcome this limitation, strategies are developed to convert acetate from the anaerobic first fermentation to the desired long chain products in a second, aerobic fermentation. For example, the acetate generated in a fermentation of *C. ljungdahlii* with syngas was converted to malate with *Aspergillus oryzae* in a second cultivation within the same fermenter (Oswald et al., 2016). Similarly, *Sporomusa ovata* was used for anaerobic acetate generation, followed by conversion to palmitate by *Acinetobacter baylyi* (Lehtinen et al., 2017). Finally, a continues process has been developed in which *Moorella thermoacetica* fixes CO_2 to acetate, which is continuously pumped into a second aerobic fermenter for conversion to triacylglycerides by *Yarrowia lipolytica* (Hu et al., 2016).

1.2. Photosynthesis

Instead of feeding hydrogen, the energy required for CO_2 reduction can also be harvested from sunlight by photosynthesis. Cyanobacteria belong to the most important photosynthetic organisms and have consequently been developed for biotechnological production of chemicals. The product spectrum at lab-scale consists of alkanes, fatty acids and fatty alcohols, terpenes, squalene, sugars, and more complex compounds (Angermayr et al., 2015; Oliver et al., 2016). The currently achieved titers have already been pushed above 1 g/l, e.g., for ethanol or 2,3 butanediol with 5.5 g/l and 3 g/l, respectively. Yet, titers are often far lower (Angermayr et al., 2015; Oliver et al., 2016). Furthermore, a separation of growth and production phase has been recommended to increase genetic stability and cultivation performance (Savakis and Hellingwerf, 2015). However, due to the low titers and productivities, competitive production with cyanobacteria might currently only be achieved for fine chemicals (Savakis and Hellingwerf, 2015). Succinate production faces particular challenges, because the cyanobacterial TCA cycle has a low activity and the conversion of 2-oxoglutarate to succinate is low (Hendry et al., 2017; Young et al., 2011; Zhang and Bryant, 2011).

1.3. Methylotrophy

Methanol is a promising candidate as energy storage compound and chemical feedstock and may form the basis of a future methanol economy (Olah, 2005). Indeed, carbon capture and utilization techniques of converting CO_2 to methanol are already in industrial use (Bansode and Urakawa, 2014; Pérez-Fortes et al., 2016; Pontzen et al., 2011; Van-Dal and Bouallou, 2013), and methanol is used as a substrate for various biotechnological fermentation processes (Clomburg et al., 2017; Looser et al., 2015; Pfeifenschneider et al., 2017; Schrader et al., 2009). For poly-hydroxybutyrate high titers of 130 g/l and productivities of 1.86 g/l/h have been reached (Kim et al., 1996). The methylotrophic yeast *Pichia pastoris* has been widely used for heterologous protein production and the metabolic capabilities are well characterized (Jorda et al., 2014; Krainer et al., 2012; Zahrl et al., 2017). Given that methylotrophic yeasts offer various advantages, like broad pH and thermotolerance, a yeast-based conversion of methanol to value added chemicals is imminent.

1.4. Synthetic carbon fixation

Implementation of (synthetic) carbon fixation pathways in naturally heterotrophic organisms offers an alternative to improving existing autotrophic strains. Examples of pathway transplantation include the reductive pentose-phosphate pathway (Antonovsky et al., 2017; Guadalupe-Medina et al., 2013; Parikh et al., 2006), methylotrophy

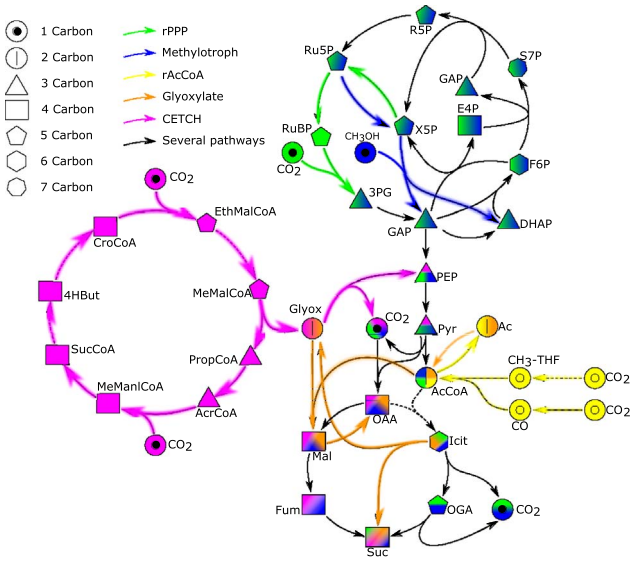

Fig. 1. Pathways of carbon fixation to succinate investigated in this study for their economic potential. The reductive pentose phosphate pathway (green), DHAP pathway of methylotrophic yeasts (blue), reductive acetyl-CoA pathway (*C. ljungdahlii*, yellow), glyoxylate shunt (*E. coli*, orange), and CETCH pathway (purple). Ac, acetate; AcCoA, acetyl-CoA; AcrCoA, acrylyl-CoA; CH3-THF, methyltetrahydrofolate; CroCoA, crotonyl-CoA; DHAP, dihydroxyacetone phosphate; EthMalCoA, ethylmalonyl-CoA; E4P, erythrose-4-phosphate; Fum, fumarate; F6P, fructose-6-phosphate; GAP, glyceraldehyde-3; Glyox, glyoxylate; Icit, isocitrate; Mal, malate; MeMalCoA, methylmalyl-CoA; MeManlCoA, methylmalonyl-CoA; OAA, oxaloacetate; OGA, 2-oxoglutarate; PEP, phosphoenol pyruvate; PropCoA, propionyl-CoA; Pyr, Pyruvate; RuBP, ribulose-bisphosphate; Ru5P, ribulose-5-phosphat; R5P, ribose-5-phosphate; Suc, succinate; SucCoA, succinyl-CoA; S7P, sedoheptulose-7-phosphate; X5P, xylulose-5-phosphate; 3PG, 3-phosphoglycerate; 4HBut, 4-hydroxyburyrate.

(Müller et al., 2015; Whitaker et al., 2017), and to a limited extend the 3-hydroxypropionate bicycle (HP-bicycle) (Cheng et al., 2016; Keller et al., 2013; Mattozzi et al., 2013). Apart from transplanting existing CO_2 fixation pathways between organisms, completely novel, synthetic pathways have been computationally screened (Bar-Even et al., 2010). Among those candidates was the crotonyl-coenzyme A (CoA)/ethylmalonyl-CoA/hydroxybutyryl-CoA (CETCH) pathway, which was subsequently selected by Schwander et al. (2016) to perform an experimental proof of principle of an artificial carbon fixation mechanism.

In this article, we evaluated the economic feasibility of microbial CO_2 conversion to succinic acid via four different metabolic pathways: (i) the reductive pentose-phosphate (Calvin-Basham-Benson) cycle, (ii) the reductive acetyl-CoA (Wood-Ljungdahl) pathway, (iii) methylotrophy in yeast, and (iv) a synthetic pathway expressed in *Saccharomyces* (Fig. 1). Based on published, physiological data or assumed metabolic or technical capabilities, we calculated maximal yields and productivities of the alternative routes using stoichiometric modeling. We further projected the capacities of CO_2 fixation pathways to industrial scale and evaluated the efficiency and profitability of the different approaches.

2. Materials and methods

2.1. Metabolic pathway selection and simulation conditions

Published genome-scale models of *Synechocystis* sp. PCC6803 (iJN678), *Clostridium ljungdahlii* ATCC 55383 (iHN637), *Escherichia coli* K-12 MG1655 (iJO1366), *Pichia pastoris* (iMT1026v3), and *Saccharomyces cerevisiae* (Yeast 7.5) were used to simulate the C_1 conversion routes shown in Fig. 1. The simulations were performed in MatlabR2017a (The Mathworks®, Inc., Natick, MA, USA) using the Flux Balance Analysis function of the COBRA toolbox 2.0 (Schellenberger et al., 2011) and Gurobi® 5 solver by maximizing a chosen objective

Table 1
Feedstock prices and cost for process requirements.

	Prize	Source
H_2	1500 EUR/t	http://heshydrogen.com/hydrogen-fuel-cost-vs-gasoline/
Glucose	450 EUR/t	http://www.indexmundi.com/commodities/?commodity=sugar&currency=eur (reference date 02/17)
Methanol	370 EUR/t	https://www.methanex.com/our-business/pricing (reference date 02/17)
Electricity cost	0.119 EUR/kW h	electricity prize in EU-28 region, http://ec.europa.eu/eurostat/statistics-explained/index.php/Energy_price_statistics (reference date 04/17)
Agitation + Aeration, $E_{t/v}$	$8.925 \cdot 10^{-4}$ EUR/l/h	Energy cost for stirred-tank reactors combined with current electricity prices (Zhuang and Herrgard, 2015)
Agitation + Aeration, $E_{t/v}$	$2.975 \cdot 10^{-4}$ EUR/l/h	Energy cost for tubular photo-bioreactors combined with current electricity prices (Jorquera et al., 2010)
Sterilization, S	$1.05 \cdot 10^{-2}$ EUR/l	Zhuang and Herrgard (2015), combined with current electricity prices

function while minimizing the taxicab norm. The non-growth associated maintenance (NGAM) demand was modeled as the hydrolysis of ATP:

$$ATP + H_2O \rightarrow ADP + H^+ + P_i \quad (1)$$

The NGAM value is typically derived by extrapolation from growth and substrate uptake rates (Varma and Palsson, 1995) and default values of the models were used for simulations of growing cells. However, it has been reported that the NGAM of non-growing cells is significantly lower (Drews and Kraume, 2007; Rebnegger et al., 2016). To account for this difference in simulations with zero growth, we calculated an NGAM from experimental data of non-growing *E. coli*, producing succinate from acetate (Li et al., 2016). The experimental acetate uptake and succinate production rate were inferred from the slope of the time profiles of metabolite concentrations of an engineered *E. coli* mutant presented in Fig. 4 of Li et al. (2016) to 1.6 $mmol/g_{CDW}/h$ (acetate) and 0.64 $mmol/g_{CDW}/h$ (succinate), respectively. These values were used as constraints for the *E. coli* model iJO1366, which was solved by Flux Balance Analysis (FBA) using the objective of maximizing the existing NGAM reaction. The resulting NGAM value was used for all simulations with non-growing cells because, in contrast to *E. coli*, knowledge of the NGAM of zero-growth during succinate production was not available for the other organisms. An explicit NGAM reaction (Eq. (1)) was missing for iJN678 (*Synechocystis*) and was added to the model. The NGAM in iJN678 carried a flux of 1.57 $mmol/g_{CDW}/h$ when optimized for biomass in autotrophic conditions.

The *Synechocystis* model iJN678 was set to carbon-limited autotrophic growth (no glucose uptake) with unconstrained photon uptake (boundary limit of 100 $mmol/g_{CDW}/h$). Unlike *Synechocystis*, *P. pastoris*, and *S. cerevisiae*, experimental substrate uptake rates were missing for *C. ljungdahlii*. To determine the substrate uptake rates for *C. ljungdahlii*, we maximized the substrate uptake rate in the genome scale model with an FBA by setting the growth yield to the experimentally observed growth phenotype observed by Straub et al. (2014) for *Acetobacterium woodii*. The use of this value is justified by the physiological similarities of *A. woodii* and *C. ljungdahlii* (Shin et al., 2016). Both are strict anaerobic, acetogenic organisms and employ the reductive acetate-CoA pathway. FBA simulations of *C. ljungdahlii* were always optimized for biomass production. Simulations of exponentially growing *E. coli* iJO1366 were performed with standard model conditions and glucose (uptake rate of 10 $mmol/g_{CDW}/h$) as growth of the mutant on acetate is not possible (Li et al., 2016). For aerobic succinate production with non-growing *E. coli*, the sole carbon source was acetate, and rates were set according to reported values (Li et al., 2016).

For simulations of *P. pastoris* the genome-scale reconstruction iMT1026v3 was used with the biomass equation for growth on methanol (Tomàs-Gamisans et al., 2017). Methanol was the limiting substrate with an uptake rate of 10 $mmol/g_{CDW}/h$, which is a realistic value in chemostats at growth rates of 0.15/h (Tomàs-Gamisans et al., 2017), while the O_2 uptake was not constrained.

The potential of the synthetic CETCH pathway (Fig. 1) (Bar-Even et al., 2010; Schwander et al., 2016) was investigated by adding the net reaction of the cycle (Eq. (2)) to the Yeast 7.5 model of *S. cerevisiae*.

$$3\,CO_2 + 7\,NADPH + 7\,H^+ + 4\,ATP + 2\,FAD \rightarrow Pyr + 7\,NADP^+ + 4\,ADP + 4\,P_i + 2\,FADH_2 \quad (2)$$

To enable the generation of reduction equivalents from hydrogen gas in this autotrophic *S. cerevisiae* strategy, a hydrogenase reaction was added to the Yeast 7.5, which reduces NAD^+ by oxidation of molecular hydrogen:

$$H_2 + NAD^+ \rightarrow NADH + H^+ \quad (3)$$

The hydrogen uptake rate was set to 30 $mmol/g_{CDW}/h$ and the CO_2 reduction rate to 10 $mmol/g_{CDW}/h$ (Mourato et al., 2017). Since the CETCH pathway utilizes NADPH, a transhydrogenase reaction was added to exchange electrons between $NADP^+$ and NAD^+:

$$NADPH + NAD^+ \rightarrow NADP^+ + NADH \quad (4)$$

Furthermore, we adapted the *S. cerevisiae* model to resemble a pyruvate decarboxylase negative strain, effective for pyruvate and reduced byproducts synthesis (van Maris et al., 2004). This was done by disabling fluxes through the pyruvate decarboxylase reaction (Yeast 7.5 reaction ID: r_0959). Growth of this strain was simulated with glucose as carbon source and aerobic conditions. A glucose uptake rate of 10 $mmol/g_{CDW}/h$ and unconstrained O_2 uptake rate (1000 $mmol/g_{CDW}/h$) were used and the objective function defined to maximize biomass formation. Additional constraints used in the FBA simulations are provided in Table 2.

2.2. Calculation of fermentation time and substrate requirements

The genome-scale models were employed to interrogate the production properties during a two-stage fermentation process (Fig. 2), in which the first stage serves to allow exponential growth from the starting biomass concentration N_0 of 0.01 g_{CDW}/l to the organism-specific final working biomass concentration N_t (Table 2). The growth rate μ of each organism was either estimated with FBA using growth as the objective function or set to experimental values taken from the literature. The duration of the exponential growth phase t_{growth} was calculated by solving Eq. (5) for t.

$$N(t) = N_0 \cdot e^{\mu \cdot t_{growth}} \quad (5)$$

To calculate volumetric resource requirements and by-product formation during the growth phase, Eq. (5) was integrated over the fermentation time (Eq. (6)) and the resulting biomass-time integral O_N multiplied with the specific consumption/production rates derived from flux distributions calculated with FBA (Eq. (7)).

$$O_N = \frac{N_0}{\mu} \cdot (e^{\mu t_{growth}} - 1) \quad (6)$$

$$c_x = v_x \cdot O_N \quad (7)$$

The variable c_x in Eq. (7) represents the concentration of metabolite '*x*' (CO_2, O_2, H_2, photons) computed as the product of the cell specific production rate (v_x) and the biomass-time integral O_N. Note, that succinate is generated only by non-growing cells. The final succinate concentration of 50 g/l (c_{Suc}, 423.7 mM) was chosen, and the produc-

Table 2
Properties for FBA simulations for the different metabolic models. The volumetric production rate of *E. coli* is an average value over the whole process.

Strain	*Synechocystis*	*C. ljungdahlii*	*E. coli*	*P. pastoris*	*S. cerevisiae*	*S. cerevisiae*
Model	iJN678[a]	iHN637[b]	iJO1366[c]	iMT1026v3[d]	Yeast 7.5[e]	Yeast 7.5[e]
Final biomass conc., g_{CDW}/L	10	2 (real.) 3 (opt.)	5.4 (real.) 49 (opt.)	10	15	50
Reference for N_t	projected	Straub et al. (2014)	calculated	optimized	projected	projected
Carbon source	CO_2	CO_2	Glc (growth), Ac (prod.)	methanol	Glc (growth), CO_2 (prod.)	Glc
Rates v, mmol/g_{CDW}/h, italics: values set as constraint, regular: simulated data						
NGAM (growth/non-growth)	1.57/ *1.36*	0.45	3.15/ *1.36*	2.51/ *1.36*	0/ *1.36*	0/ *1.36*
Carbon	*4* (growth), *0.5*[f] (prod., real.), *4*[a] (prod., opt.)	*31.5*[g] (real.), *66.5* (opt.)	*10* (Glc), *1.6*[h] *(Ac, real.)* *10*[i] *(Ac, opt.)*	*10*	*10* (Glc) *10*[i] (CO_2)	*10* (Glc, growth), *1*[k] (Glc, prod.)
H_2/photons	59 (growth), 6/38 (prod. real./opt.)	63.7 (real.), 135.2 (opt.)	–	–	30 26.7 (real.) 30 (opt.)	–
O_2	6 *(produced)*	*0 (anaerobic)*	0.96/4.1 (prod., real./opt.)	9.4/6.3 (prod., real./opt.)	4.6/5.2 (prod., real./opt.)	0.75
Acetate/Succinate	0.125 (real.), 1 (opt.)	15 (Ac, real.), 30 (Ac, opt.)	0.64 (real.), 4.53 (opt.)	0.625 (real.), 2.5 (opt.)	0.625 (real.), 2.5 (opt.)	1.5
Growth rate, simulated/h	0.1	0.05 (real.) 0.15 (opt.)	0.98	0.12	0.95	0.95
Acetate/succinate productivity, g/l/h	0.15 (real.) 1.2 (opt.)	3.5 (real.) 10.6 (opt.)	0.8 (real.) 2.6 (opt.)	0.7 (real.) 3 (opt.)	1.1 (real.) 4.4 (opt.)	8.9

Scenario: real.-realistic; opt.-optimistic; prod., production phase; Glc, glucose; Ac, acetate.
[a] Nogales et al. (2012).
[b] Nagarajan et al. (2013).
[c] Orth et al. (2011).
[d] Tomas-Gamisans et al. (2016).
[e] Aung et al. (2013).
[f] Gong et al. (2015).
[g] Straub et al. (2014).
[h] Li et al. (2016).
[i] Zhao and Shimizu (2003).
[j] Mourato et al. (2017).
[k] Diderich et al. (1999).

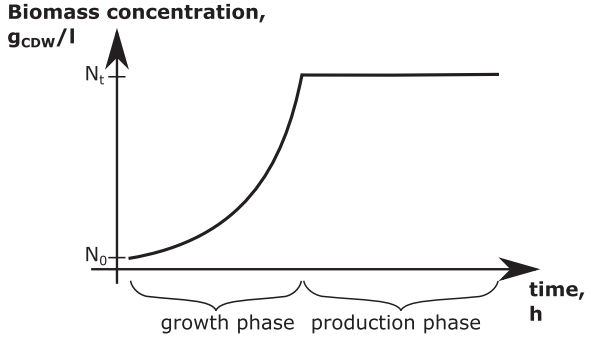

Fig. 2. Idealized process of a two-stage fermentation of succinate production. During the growth phase, the cells exponentially grow from an initial biomass concentration N_0 to the final working biomass concentration N_t. Succinate production takes place after cessation of growth.

tion time t_{Pro} was calculated based on a constant biomass concentration N_t and the specific succinate production rate v_{Suc}:

$$t_{Pro} = \frac{c_{Suc}}{v_{Suc} \cdot N_t} \tag{8}$$

The succinate specific production rate (v_{Suc}) was computed by FBA with the genome-scale models described in Section 2.1, constrained by the carbon uptake rates given in Table 2 and optimized for succinate production.

Succinate production via the reductive acetyl-CoA pathway was simulated with a 2-organism/2-fermenter concept, in which acetate produced autotrophically by *C. ljungdahlii* was converted aerobically in a second fermentation by *E. coli*. Acetate production with *C. ljungdahlii* was assumed to take place during both growth and stationary phase. *E. coli* was rapidly pre-cultured on glucose, assuming optimal biomass accumulation without byproducts and was present at constant biomass densities in the second downstream fermenter. The one-stage fermentation of *C. ljungdahlii* was rate limiting while the aerobic acetate to succinate conversion rate by *E. coli* was controlled by the *E. coli* biomass density and was matched to the acetate production rate. The production time included accumulation of acetate by *C. ljundgahlii* and succinate by *E. coli*. Experimental evidence showed an acetate to succinate conversion efficiency in *E. coli* of 80% (Li et al., 2016). Therefore, the overall amount of acetate required was set to 62.5 g/l (1059.3 mmol/l). The procedure to determine the overall fermentation time was as follows:

(1) the biomass-time integral O_N^{Prod} (g_{CDW}h/l) required to generate the target acetate concentration was calculated with Eq. (7) using a time-invariant acetate production rate of 14.65 mmol/g_{CDW}/h and 30 mmol/g_{CDW}/h for a realistic and an optimistic scenario, respectively.
(2) The duration of the exponential growth phase t_{growth} was determined with Eq. (5) assuming a constant working biomass concentration of N_t = 2 g_{CDW}/l.
(3) The biomass-time integral of the exponential growth phase was calculated with Eq. (6).

$$O_N^{Tot} = O_N^{Growth} + O_N^{Prod} \tag{9}$$

(4) The overall biomass-time integral O_N^{Tot} was determined with Eq. (9).
(5) The total process duration was calculated with Eq. (10), in which

the second term defines the duration of the production phase and N_t the working biomass concentration.

$$t_{tot} = t_{Growth} + \frac{O_N^{Prod}}{N_t} \tag{10}$$

The steps (1)–(5) were combined to give Eq. (11):

$$t_{tot} = \frac{\ln\left(\frac{N_t}{N_0}\right)}{\mu} + \frac{\frac{c_{Ac}}{v_{Ac}} - \frac{N_0}{\mu}\cdot(e^{\mu\cdot t_{growth}} - 1)}{N_t} \tag{11}$$

2.3. Cost calculations and sensitivity analysis

The calculated costs were normalized to the final succinate concentration. The two-fermenter strategy employing *C. ljungdahlii* and *E. coli*, was designed as a retentostat with a constant outflow of the succinate-containing, cell-free fermentation broth. In this scenario, we used the amount of succinate produced relative to the biomass concentrations and fermenter volumes of *C. ljungdahlii* and the *E. coli* instead of the absolute succinate concentration. Process duration, biomass concentrations, and feedstock requirements to synthesize the target volumetric succinate amount of 50 g/l were calculated as described in Section 2.2. Table 1 shows process and commodity prices used for the calculations.

The total volumetric succinate production costs $Cost_{Suc}$ comprised the demand of substrates ($Cost_{Sub}$), energy per time and per volume ($E_{t/V}$), and sterilization per volume (S) (Eq. (12)) and was divided by the succinate concentration to yield the overall costs per metric ton succinate (P_{Suc}, Eq. (13)).

$$Cost_{Suc} = Cost_{Sub} + E_{t/V}\cdot t_{tot} + S \tag{12}$$

$$P_{Suc} = \frac{Cost_{Suc}}{c_{Suc}} \tag{13}$$

The expenditures for the substrates, H_2, methanol or glucose, were calculated using Eq. (14).

$$Cost_{Sub} = \frac{c_{Sub}\cdot M_{Sub}}{1\cdot 10^6}\cdot price_{Sub} \tag{14}$$

c_{Sub} was calculated using Eq. (7). M_{Sub} is the molar mass, and $price_{Sub}$ the substrate price given in Table 1.

The volumetric agitation and aeration costs were obtained by multiplying the energy demands from literature (Table 1) with the total fermentation time (Table 3).

The cyanobacterial strategy was defined to be operated with sunlight assuming 10 h per day of sufficient irradiation for CO_2 fixation. Succinate production was assumed to only take place in the period of CO_2 fixation and because of the optimization towards succinate all carbon is converted to the product of interest. However, this is a simplification of the actual metabolic processes and furthermore metabolic activities in the dark were accounted for by calculating costs for agitation and aeration, required to maintain viable conditions, over the total fermentation time.

2.4. Additional calculations for the two-organism/two-fermenter strategy

The proposed *C. ljungdahlii/E. coli* strategy used two connected fermentations, each equipped with cell retention, in which the medium from the first fermenter is continuously fed into the aerated second fermenter. Variation of the reactor volume V (l) and the dilution rate of the *C. ljungdahlii* fermentation $D = \frac{q}{V^{Clju}}$ (1/h), with q being the volume flow rate (l/h), affects the acetate concentration, which in turn requires adaptation of the *E. coli* biomass concentration in the second fermenter to guarantee complete and immediate acetate conversion. The concentration of acetate in the *C. ljungdahlii* fermenter was calculated via Eq. (15).

$$\frac{dc_{Ac}^{Clju}}{dt} = v_{Ac}^{Clju}\cdot N_t^{Clju} - D^{Clju}\cdot c_{Ac}^{Clju} = 0$$
$$c_{Ac}^{Clju} = \frac{v_{Ac}^{Clju}\cdot N_t^{Clju}}{D^{Clju}} = \frac{APRn}{D^{Clju}} \tag{15}$$

The subscript index Ac and the superscript index Clju denote acetate and *C. ljungdahlii*, respectively. The volume flow rate is equal in both coupled fermenters. The variable APRn represents the volumetric molar acetate production rate (mmol/l/h).

The biomass of *E. coli* N_t^{Ecol} required to fully convert the incoming acetate was determined with Eq. (16). The superscript Ecol stands for *E. coli*. N_t^{Ecol} is a function of the volume ratio of the *C. ljungdahlii* – *E. coli* fermenters, which was varied between 1 and 20 in the sensitivity analysis while the APRn was kept constant.

$$\frac{dc_{Ac}^{Ecol}}{dt} = D^{Ecol}\cdot c_{Ac}^{Clju} - v_{Ac}^{Ecol}\cdot N_t^{Ecol} - D^{Ecol}\cdot c_{Ac}^{Ecol} = 0$$
$$\text{with } c_{Ac}^{Ecol} \approx 0$$
$$N_t^{Ecol} = \frac{V^{Clju}}{V^{Ecol}}\cdot\frac{APRn}{v_{Ac}^{Ecol}} \tag{16}$$

The concentration of succinate v_{Suc}^{Ecol} in the fermentation broth released from the *E. coli* fermenter during the steady state production phase was determined with Eq. (17).

$$\frac{dc_{Suc}}{dt} = v_{Suc}^{Ecol}\cdot N_t^{Ecol} - D^{Ecol}\cdot c_{Suc}^{Ecol} = 0$$
$$c_{Suc} = \frac{v_{Suc}^{Ecol}\cdot N_t^{Ecol}}{D^{Ecol}} \tag{17}$$

In the realistic and optimistic scenarios, we assumed a dilution rate $\frac{q}{V^{Ecol}}$ of 10/h, which corresponds to the condition that the volume flow rate is 10-fold the reactor volume. This dilution rate is high, but still in

Table 3
Properties of the simulated strategies with a target succinate concentration of 50 g/l and for the optimistic scenario. Substrate requirements were calculated as the sum of growth and production phase according to Eqs. (10) and (11). Because *E. coli* growth on glucose is rapid, we assumed it to take place within the *C. ljundgahlii* growth phase. Cell densities and productivities were according to the optimistic scenarios in Table 2 and black stars in Fig. 3. Parameters of cost calculation are shown in Table 1. Glc, Glucose.

Strategy	*Synechocystis*	*C. ljungdahlii* – *E. coli*	*P. pastoris*	*S. cerevisiae*	*S. cerevisiae* (Glucose)
growth phase + production time, h	73 + 42 = 115	38 + 5 = 43	56 + 17 = 73	8 + 11 = 19	9 + 6 = 15
overall product yield, C-mol/C-mol	81%	72%	68%	64%	35%
product yield during production, C-mol/C-mol$_{Carbon}$	100%	72%	100%	100%	100%
Substrate cost EUR/l	–	$1.4\cdot10^{-2}$ (H_2) $2\cdot10^{-3}$ (Glc)	$3\cdot10^{-2}$ (MeOH)	$1.3\cdot10^{-2}$ (H_2) $1.3\cdot10^{-1}$ (Glc)	$6.6\cdot10^{-2}$ (Glc)
Energy cost EUR/l	0.1	$4\cdot10^{-2}$	$6.5\cdot10^{-2}$	$1.7\cdot10^{-2}$	$1.3\cdot10^{-2}$
rel. substrate cost	0%	28%	32%	49%	74%
Production cost EUR/t (50 g/l)	1847	1136	2107	1078	1785
Production cost EUR/t (100 g/l)	1226	828	1405	776	1172

the order of achievable rates reported, for example, for immobilized cells (Qureshi et al., 2005).

The energy requirement of the *C. ljungdahlii – E. coli* fermentation is a function of the two fermenter volumes. For *E. coli*, the volume of the *E. coli* fermenter is inversely proportional to the biomass concentration according to Eq. (16). The total energy requirement is calculated by combining Eq. (16) with the total fermentation time and volumes as derived from Eq. (18):

$$E_{tot}^{Clju} = t_{tot} \cdot E_{t/V} \cdot \frac{V_{Clju} + V_{Ecol}}{V_{Clju}}$$

$$E_{tot}^{Clju} = t_{tot} \cdot E_{t/V} \cdot \left(1 + \frac{APRn}{v_{Ac}^{Ecol} \cdot N_t^{Ecol}}\right) \quad (18)$$

3. Results

3.1. Definition of realistic and optimistic simulation scenarios

We tested the succinate productivity of five different production strategies: (i) light driven CO_2 fixation in cyanobacteria, (ii) anaerobic CO_2 reduction to acetate by *C. ljungdahlii* and subsequent aerobic conversion of acetate to succinate by *E. coli*, (iii) methanol conversion to succinate by *P. pastoris*, (iv) synthetic CO_2 reduction pathway in *S. cerevisiae*, and (v) a heterotrophic succinate production from glucose in *S. cerevisiae*. The simulations were performed in two contexts: 'realistic' parameter sets, based on experimental data or assumed to be achievable without substantial metabolic or process engineering efforts; and 'optimistic' parameter sets that require extensive genetic modifications. We based our analysis on the production of a succinate titer of 50 g/l, which is within the tolerance range of most organisms and lower than maximum concentrations currently reached (Cui et al., 2017; Zhu et al., 2014), but we also tested price levels with final titers of 100 g/l.

The realistic and optimistic scenarios are specific for each strategy and represent key properties of the production. In the cyanobacterial strategy, the difference between the scenarios was the CO_2 uptake rate. In the *C. ljungdahlii/E. coli* strategy, we defined the optimistic scenario as having a doubled specific acetate production rate, a tripled growth rate and higher maximum biomass concentration for *C. ljungdahlii* compared to the realistic scenario, which was based on published experimental data (Straub et al., 2014). For *E. coli*, the specific acetate uptake was increased six-fold from the realistic case (Li et al., 2016) to the optimistic case. The realistic scenarios of *P. pastoris* and *S. cerevisiae* strategies were based on a 25% yield (C-mol/C-mol) on carbon source while carbon was fully converted to succinate in simulations of the optimistic scenario.

3.2. Succinate productivity and cost assessment

An important benchmark for the economic viability of bio-based succinate production is the volumetric productivity, which should surpass 2.5 g/l/h, according to estimates of the U.S. Department of Energy (Werpy et al., 2004). We determined the volumetric productivity for the succinate producing fermentation period, i.e. the production phase of the two-stage fermentations and the total time of the one-stage fermentation. Whereas this limit was not met by any strategy for the realistic constraints, most strategies exceeded the productivity limit in the optimistic scenario, except of the cyanobacterial strategy (Table 2). An additional noteworthy point are the high carbon uptake rates in the *C. ljungdahlii* strategy (> 60 mmol/g_{CDW}/h, optimistic scenario). The accordingly high molecular hydrogen uptake rate of the strain (> 130 mmol/g_{CDW}/h, optimisitic scenario) will require specialized bioreactors allowing very high k_La values, for example hollow-fiber membrane reactors for which mass transfer coefficients above 100/h have been reported (Orgill et al., 2013), and pressurized systems to increase the H_2 solubility (Phillips et al., 2017).

The production times required to achieve a succinate titer of 50 g/l varied greatly, from 42 h for the cyanobacterial strategy to 11 h for the yeast-based process relying on the synthetic CETCH pathway (Table 3). Note, that with the *C. ljungdahlii/E. coli* strategy succinate is produced already during the growth phase of *C. ljungdahlii*. For slow growing organisms like the cyanobacteria and *C. ljungdahlii*, but also *P. pastoris* growing on methanol, the exponential growth phase to reach the final biomass concentration was a large contributor to the total fermentation time. The growth phase was shortest for *S. cerevisiae* expressing the CETCH pathway, but still comprised approximately 60% of the overall fermentation time. The overall product yield on assimilated and dissimilated carbon was greatest for the cyanobacterial strategy (80% (C-mol/C-mol)), hence carbon substrate requirements were lowest. The synthetic carbon fixation in *S. cerevisiae* had the lowest yield, which, however, was still higher than that of the heterotrophic strategy using glucose (Table 3).

The most cost effective autotrophic production was achieved with the engineered *S. cerevisiae* strategy, which is explained by the low H_2 cost, and the low energy requirement due to the short process time resulting in production costs of 1078 EUR/t. Note, however, that the accumulation of biomass during exponential phase is fueled by glucose (Table 3, see Material and Method section for details on the calculations). The two-stage fermentation of *C. ljungdahlii – E. coli* was similarly cost-effective. The highest cost was estimated for the *P. pastoris* strategy because of the high methanol price, which contributed half of the production cost. Also, the long fermentation time resulted in a high energy demand. Compared with a conventional fermentation of *S. cerevisiae* with glucose, the strategies employing methanol-driven *P. pastoris* and light-driven cyanobacteria were more expensive.

We also tested performance with an increased final titer of 100 g/l instead of 50 g/l. The associated, reduced volumetric costs were most prominent for the *P. pastoris* strategy, for which the expenses dropped by 33% to 1405 EUR/t. This saving is generated due to the reduced fraction of carbon used for the synthesis of biomass, the concentration of which was kept constant. Note, however, that downstream processing and investments costs are excluded from the analysis. The downstream cost will be similar for cyanobacteria, *P. pastoris*, and *S. cerevisiae* strategies because of identical final succinate titers. The *C. ljungdahlii/E. coli* two-step strategy, by contrast, is an open system with a constant outflow of a more dilute succinate concentration, which will ultimately raise the product purification cost.

3.3. Sensitivity of production cost to the biomass concentration of the microbial host

Higher biomass concentrations do not by default increase profitability. A trade-off exists between high volumetric productivities requiring high biomass concentrations (denominator of Eq. (8)) and substrate costs, which increase with the biomass concentration (Eqs. (5)–(7)). In addition, higher biomass concentrations require a longer growth phase. Consequently, the biomass concentration is a parameter that needs to be optimized to minimize both overall production time and costs. We calculated the overall production cost for a broad range of possible biomass concentrations to evaluate the sensitivity of the production cost to changes of this parameter (Fig. 3). A hyperbolic, decreasing trend of production costs for increasing biomass concentrations of cyanobacteria and *S. cerevisiae* was observed and biomass concentrations above 10 g/l resulted only in marginal savings of the production cost. Overall production costs of the *P. pastoris* based process dropped with increasing biomass because of a stark decrease of the energetic costs but increased again because of the increasing substrate expenses (Fig. 3C). For a biomass concentration of 10 g_{CDW}/l, the production rate exceeded the 2.5 g/l/h threshold and was therefore chosen for the cost analysis.

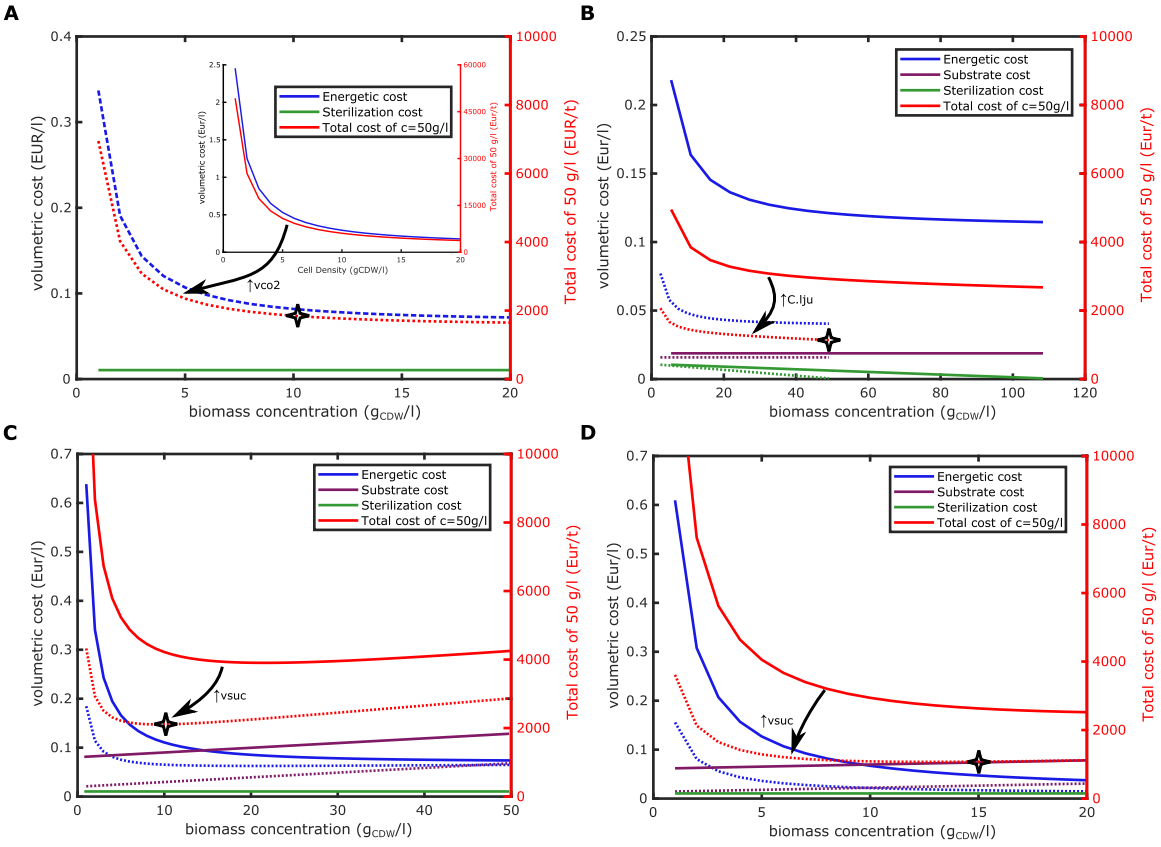

Fig. 3. Dependence of volumetric costs for energy, substrate, and sterilization, and the total cost to produce 1 t succinate on the biomass concentration. Calculations were based on a final succinate titer of 50 g/l. Lines represent results for the realistic scenario, and dashed lines represent the optimistic scenario. The black stars denote the optimal process conditions listed in Tables 2 and 3. (A) succinate production from sunlight, CO_2 and water with cyanobacteria for the realistic scenario and improvements following increased CO_2 uptake (v_{CO2}) in the optimistic scenario, the inlet figure shows the total costs above 45,000 Eur/t, (B) *C. ljungdahlii – E. coli* strategy with CO_2 fixation to acetate via the reductive acetyl-CoA pathway and conversion to succinate by *E. coli*. Here, biomass concentration refers to *E. coli*, which can be varied by simultaneously adjusting the volume ratios of the two concomitant fermenters, (C) conversion of methanol to succinate by methylotrophic yeast, the optimistic scenario is achieved by increasing the succinate yield and productivity (v_{suc}), D) CO_2 fixation via the synthetic CETCH pathway in *S. cerevisiae*, again the optimistic scenario is achieved by increasing the succinate yield and productivity (v_{suc}).

The *C. ljungdahlii – E. coli* fermentation had the most variable operating parameters. Because acetate formation by *C. ljungdahlii* was the rate limiting step, changes in the *E. coli* biomass concentration did not affect the overall process time. However, at a higher *E. coli* biomass concentration a smaller bioreactor volume is required, which in turn reduces the energy expenses for agitation and aeration, as well as the volume-specific sterilization requirements. We set the lowest fermenter volume for *E. coli* to 5% of the *C. ljungdahlii* fermenter volume. The derivation of the energy cost is shown in Eq. (18) and leads to an inverse proportionality of the energy and *E. coli* biomass (Fig. 3B).

We examined in more detail the sensitivity of the acetate production time in the *C. ljungdahlii* fermentation to changes of the parameters growth rate, biomass concentration, and specific acetate production rate (Fig. 4). The highest impact on the acetate synthesis rate was observed by increasing the growth rate of *C. ljungdahlii,* because the growth phase was disproportionally large compared to the overall fermentation time. A further reduction of the production time was achieved by substantially and simultaneously increasing the specific acetate production rate from 14 mmol/g_{CDW}/h to nearly 30 mmol/g_{CDW}/h, resulting in a reduction of the overall production time from 125 h to less than 50 h (red star, Fig. 4B). In contrast, increasing the biomass concentration of *C. ljungdahlii* had a limited impact on lowering the total production time and even became detrimental when the specific acetate production rate was concurrently increased (Fig. 4C).

4. Discussion

Here, we analyzed the performance of different CO_2 to succinate conversion strategies and evaluated the conditions required for an economically viable process. With production costs in the range of 1100–2100 EUR/t (Table 3), the costs of succinic acid from CO_2 and methanol are comparable to glucose-based bioprocesses. The most cost-effective processes are achievable with the strategies involving acetogens (*C. ljungdahlii/E. coli*) and the engineered carbon-fixing *S. cerevisiae*, whereas expenses are higher for the cyanobacterial and methylotrophic strategy. Our assessment of production costs also support the results of Comer et al. (2017) that the biggest contributor to the expense for the methylotrophic strategy is the methanol price, for which we had chosen the current market price (Table 1). CO_2 conversion to methanol is already conducted in conditions with cheap electricity and proximity to CO_2 intense industries (Carbon Recycling Inc, BASF), and the future methanol price is expected to decrease to 100 EUR/t (Pfeifenschneider et al., 2017), i.e., to nearly one quarter of the current price. That being the case, the production cost of the methylotrophic strategy would decrease to 1100–1600 EUR/t succinic acid.

All evaluated strategies require substantial optimization of the strain performance to increase production rates to the limit of commercial competitiveness (Fig. 5). The blue circles in Fig. 5 indicate that production rates achievable with standard metabolic optimization (i.e., optimization of co-factor supply, suppression of competitive reaction pathways) that mainly affect the product yield are insufficient because productivities would remain below the minimum of 2.5 g/l/h defined by the US Department of Energy (Fig. 5, green circles) (Werpy et al., 2004). Our simulations have shown that high-cell density fermentations can increase volumetric productivity but do not result

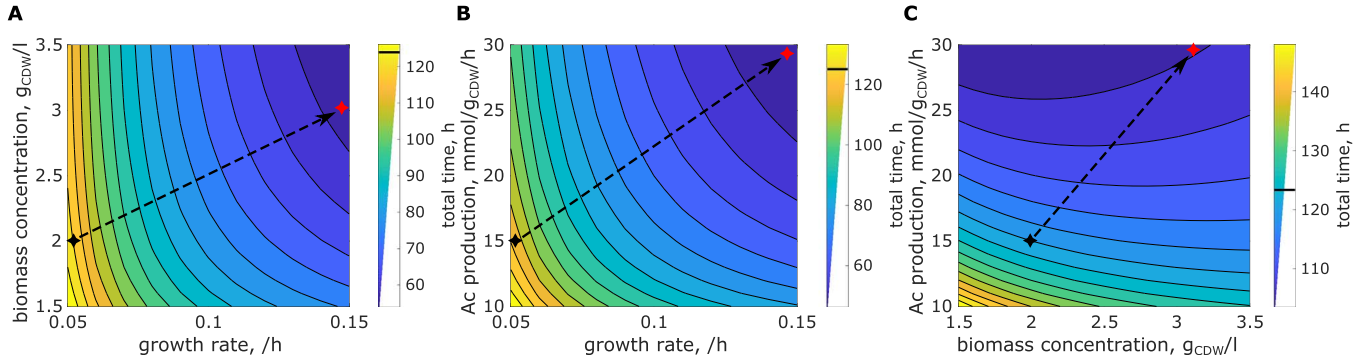

Fig. 4. Sensitivity of the total time of the *C. ljungdahlii* fermentation to the growth rate and biomass concentration (A), growth rate and specific acetate production (B), and biomass concentration and specific acetate production rate (C). The calculation of the data is based on Eq. (11). The currently achievable status is marked with a black star and a black line for the total acetate production time; the future optimization potential is indicated with a red star. Each subfigure shows the improvement of the total time for two variables; for the optimistic scenario all three variables were increased.

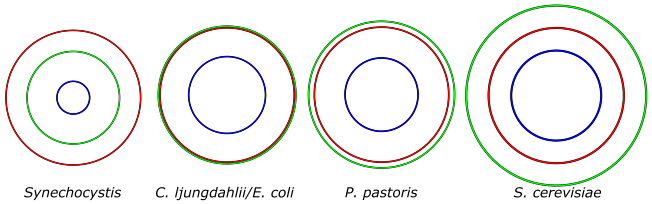

Fig. 5. Production capacities of the four strategies cyanobacterial, *C. ljungdahlii – E. coli*, *P. pastoris* and *S. cerevisiae*. The current productivity is shown by blue lines, the realistic-optimistic production is marked by a green, and the minimum production for economic viability of 2.5 g/l/h (Werpy et al., 2004) by a red line.

in a reduction of overall production costs because of reduced overall product yield and consequently increased substrate costs. Rather, significant research must be devoted to optimize the substrate uptake and succinate production rates of the simulated optimistic scenarios to achieve economic succinate production from C1 carbon sources.

One major drawback of the cyanobacteria-based process is the low specific carbon uptake and fixation rate at increased biomass concentrations, which needs to be addressed to elevate the productivity. The carbon uptake rate of cyanobacterial fermentations is generally high during the initial growth rate, but decreases at steady state when biomass concentrations of approx. 3 g_{CDW}/l are reached (Zhang et al., 2015). The decrease in carbon uptake is probably caused by shadow-casting of cells at higher biomass concentrations resulting in photon-limited growth. This condition is accounted for in the realistic scenario, in which the carbon uptake has been limited to experimental rates of 0.5 mmol/g_{CDW}/h (Gong et al., 2015) and photon fluxes to 6 mmol/g_{CDW}/l (Table 2). To increase the carbon uptake at high biomass concentrations, new bioreactor designs are required. We have simulated the cyanobacterial strategy assuming steady metabolism during the assumed 10 h of sunlight, during which all carbon is converted into succinic acid, and no metabolic activity in the dark. A more realistic representation of a cyanobacterial strategy requires the more accurate inclusion of diurnal cycles with different rates of production. Consequently, the predictions for cyanobacteria might be particularly optimistic and the effective potential of the cyanobacterial process be lower than reported here (Knoop and Steuer, 2015; Savakis and Hellingwerf, 2015).

Similarly, the *C. ljungdahlii* fermentation is limited by the transfer rate of the energy carrier H_2 in the realistic scenario and significantly elevated gas transfer rates are required to increase the productivity beyond the productivity limit. Such an increase can be achieved by using pressurized systems along with an optimization of the bioreactor configuration for improved gas mass transfer (k_La) (Kantzow et al., 2015; Orgill et al., 2013). Further potential bottlenecks caused by enzymatic capacities need to be identified and targeted by metabolic or protein engineering. Optimization of acetate production in *C. ljungdahlii* is demanding because acetate production is coupled to growth with the consequent use of acetyl-CoA for anabolism (Abubackar et al., 2015; Cotter et al., 2009). Hence, achieving higher yields of acetate production requires complex deregulation and decoupling from cell growth.

The methylotrophic yeast *P. pastoris* is a model organism, for which a range of genetic engineering tools exist facilitating metabolic engineering efforts. The most important genetic modifications are likely to be associated to the engineering of a switch that changes the metabolic objective from growth to succinic acid production, while still maintaining high metabolic fluxes. Difficulties in enabling this transition has led Klamt et al. (2017) to conclude that two-stage fermentations are not outperforming one-stage fermentation strategies. However, in some organisms nitrogen limitation causes growth arrest while C-sources are still metabolized at high rate (Zambanini et al., 2016). Also, *E. coli* has been manipulated to show high glucose throughput in resting conditions (Michalowski et al., 2017), thus enabling more favorable two-stage fermentation strategies. The *P. pastoris* strategy had in our simulations a very long growth phase, because it was assumed to take place with methanol. Adaptive laboratory evolution to select faster growing mutants or the use of alternative methylotrophic organisms with higher growth rates, e.g., *Pseudomonas methylotropha* (*Methylobacillus glycogenes*) (Goldberg et al., 1976) might overcome this barrier.

The biotechnological use of synthetic autotrophic *S. cerevisiae* is very promising but still years away. The stable integration of more than twenty heterologous genes and expression of the encoding heterologous enzymes in active form is a great molecular biology challenge. Furthermore, the expression levels and reaction fluxes must be fine-tuned and harmonically integrated into the host metabolism. The feasibility of the synthetic autotrophs would have to be re-evaluated once the basic challenges of synthetic transplantation of trophic modes is solved.

The basic economic analysis of autotrophic succinic acid production conducted here was based on minimal input of experimental data and excluded downstream processing and investment costs. Further, more detailed economic evaluations are necessary to evaluate sustainability and competitiveness similar to Zhuang and Herrgard (2015) who included land use, and agricultural features of the feedstock, impact of the energy and market sector, metabolic details of the applied strain and process designs. If similarly adapted for autotrophic succinic acid production, it is possible to more precisely identify optimal environmental and regulatory application niches.

5. Conclusion

The evaluation of the economic performance of microbial conversion of CO_2 to succinate is an important step in identifying the most

applicable solutions and the knowledge and engineering gaps that have to be addressed (Köhler et al., 2015). The applied FBA-based method quantitatively explores the metabolic capabilities based on technical and physiological constraints and thus allows a first screening and evaluation of process alternatives at very early development stages, at which no detailed data and insight is available.

Whereas conventional petrochemical and fermentative succinic acid production based on glucose will provide the bulk of succinic acid because of ubiquitous substrate availability, simple process design and high productivities, our analysis suggests that also CO_2 can be a sustainable feedstock for succinic acid production if readily available or efficiently being converted to methanol, and if technical barriers such as limiting gas transfer rates or shadow-casting in photo-bioreactors can be overcome.

Acknowledgements

The authors thank Ahmed Zahoor ul-Hassan and Jörg Mampel for stimulating discussions and Katja Bühler for discussions on cyanobacterial production processes. Tobias B. Alter supplied valuable feedback for corrections on the manuscript.

Funding

This work was supported by the Biotechnology Research and Information Network AG (BRAIN AG) and by the German Federal Ministry of Education and Research (BMBF) as part of the Strategic Alliance Zero Carbon Footprint (Grant no. FKZ 031A217F).

Appendix A. Supplementary material

Supplementary data associated with this article can be found in the online version at doi:10.1016/j.mec.2018.e00075.

References

Abubackar, H.N., Veiga, M.C., Kennes, C., 2015. Ethanol and acetic acid production from carbon monoxide in a *Clostridium* strain in batch and continuous gas-fed bioreactors. Int J. Environ. Res. Public Health 12 (1), 1029–1043.

Ahn, J.H., Jang, Y.-S., Lee, S.Y., 2016. Production of succinic acid by metabolically engineered microorganisms. Curr. Opin. Biotechnol. 42, 54–66.

Ampelli, C., Perathoner, S., Centi, G., 2015. CO_2 utilization: an enabling element to move to a resource- and energy-efficient chemical and fuel production. Philos. Trans. R. Soc. A 373 (2037), 20140177.

Angermayr, S.A., Rovira, A.G., Hellingwerf, K.J., 2015. Metabolic engineering of cyanobacteria for the synthesis of commodity products. Trends Biotechnol. 33 (6), 352–361.

Antonovsky, N., Gleizer, S., Milo, R., 2017. Engineering carbon fixation in *E. coli*: from heterologous RuBisCO expression to the Calvin–Benson–Bassham cycle. Curr. Opin. Biotechnol. 47, 83–91.

Aung, H.W., Henry, S.A., Walker, L.P., 2013. Revising the representation of fatty acid, glycerolipid, and glycerophospholipid metabolism in the consensus model of Yeast metabolism. Ind. Biotechnol. 9 (4), 215–228.

Bansode, A., Urakawa, A., 2014. Towards full one-pass conversion of carbon dioxide to methanol and methanol-derived products. J. Catal. 309, 66–70.

Bar-Even, A., Noor, E., Lewis, N.E., Milo, R., 2010. Design and analysis of synthetic carbon fixation pathways. Proc. Natl. Acad. Sci. USA 107 (19), 8889–8894.

Becker, J., Lange, A., Fabarius, J., Wittmann, C., 2015. Top value platform chemicals: bio-based production of organic acids. Curr. Opin. Biotechnol. 36, 168–175.

Bozell, J.J., Petersen, G.R., 2010. Technology development for the production of biobased products from biorefinery carbohydrates – the US Department of Energy's "Top 10" revisited. Green Chem. 12 (4), (539-539).

Cheng, Z., Jiang, J., Wu, H., Li, Z., Ye, Q., 2016. Enhanced production of 3-hydroxypropionic acid from glucose via malonyl-CoA pathway by engineered *Escherichia coli*. Bioresour. Technol. 200, 897–904.

Choi, S., Song, C.W., Shin, J.H., Lee, S.Y., 2015. Biorefineries for the production of top building block chemicals and their derivatives. Metab. Eng. 28, 223–239.

Clomburg, J.M., Crumbley, A.M., Gonzalez, R., 2017. Industrial biomanufacturing: the future of chemical production. Science 355 (6320), aag0804.

Comer, A.D., Long, M.R., Reed, J.L., Pfleger, B.F., 2017. Flux balance analysis indicates that methane Is the lowest cost feedstock for microbial cell factories. Metab. Eng. Comm. 5, 26–33.

Cotter, J.L., Chinn, M.S., Grunden, A.M., 2009. Ethanol and acetate production by *Clostridium ljungdahlii* and *Clostridium autoethanogenum* using resting cells. Bioprocess Biosyst. Eng. 32 (3), 369–380.

Cui, Z., Gao, C., Li, J., Hou, J., Lin, C.S.K., Qi, Q., 2017. Engineering of unconventional yeast *Yarrowia lipolytica* for efficient succinic acid production from glycerol at low pH. Metab. Eng. 42, 126–133.

Daniell, J., Köpke, M., Simpson, S., 2012. Commercial biomass syngas fermentation. Energies 5 (12), 5372–5417.

Diderich, J.A., Schepper, M., van Hoek, P., Luttik, M.A.H., van Dijken, J.P., Pronk, J.T., Klaassen, P., Boelens, H.F.M., de Mattos, M.J.T., van Dam, K., et al., 1999. Glucose uptake kinetics and transcription of HXTGenes in chemostat cultures of *Saccharomyces cerevisiae*. J. Biol. Chem. 274 (22), 15350–15359.

Drews, A., Kraume, M., 2007. On maintenance models in severely and long-term limited membrane bioreactor cultivations. Biotechnol. Bioeng. 96 (5), 892–903.

Dürre, P., Eikmanns, B.J., 2015. C1-carbon sources for chemical and fuel production by microbial gas fermentation. Curr. Opin. Biotechnol. 35, 63–72.

Fast, A.G., Papoutsakis, E.T., 2012. Stoichiometric and energetic analyses of non-photosynthetic CO_2-fixation pathways to support synthetic biology strategies for production of fuels and chemicals. Curr. Opin. Chem. Eng. 1 (4), 380–395.

Goldberg, I., Rock, J.S., Benbassat, A., Mateles, R.I., 1976. Bacterial yields on methanol, methylamine, formaldehyde, and formate. Biotechnol. Bioeng. 18 (12), 1657–1668.

Gong, F., Liu, G., Zhai, X., Zhou, J., Cai, Z., Li, Y., 2015. Quantitative analysis of an engineered CO_2-fixing *Escherichia coli* reveals great potential of heterotrophic CO_2 fixation. Biotechnol. Biofuels 8 (1), 1–10.

Guadalupe-Medina, V., Wisselink, H., Luttik, M.A.H., de Hulster, E., Daran, J.M., Pronk, J.T., van Maris, A.J.A., 2013. Carbon dioxide fixation by Calvin-cycle enzymes improves ethanol yield in yeast. Biotechnol. Biofuels 6 (1), (125-125).

Hendry, J.I., Prasannan, C., Ma, F., Möllers, K.B., Jaiswal, D., Digmurti, M., Allen, D.K., Frigaard, N.-U., Dasgupta, S., Wangikar, P.P., 2017. Rerouting of carbon flux in a glycogen mutant of cyanobacteria assessed via isotopically non-stationary ^{13}C metabolic flux analysis. Biotechnol. Bioeng. 114 (10), 2298–2308.

Hu, P., Chakraborty, S., Kumar, A., Woolston, B., Liu, H., Emerson, D., Stephanopoulos, G., 2016. Integrated bioprocess for conversion of gaseous substrates to liquids. Proc. Natl. Acad. Sci. USA 113 (14), 3773–3778.

Jansen, M.L.A., van Gulik, W.M., 2014. Towards large scale fermentative production of succinic acid. Curr. Opin. Biotechnol. 30, 190–197.

Jorda, J., de Jesus, S.S., Peltier, S., Ferrer, P., Albiol, J., 2014. Metabolic flux analysis of recombinant *Pichia pastoris* growing on different glycerol/methanol mixtures by iterative fitting of NMR-derived ^{13}C-labelling data from proteinogenic amino acids. New Biotechnol. 31 (1), 120–132.

Jorquera, O., Kiperstok, A., Sales, E.A., Embirucu, M., Ghirardi, M.L., 2010. Comparative energy life-cycle analyses of microalgal biomass production in open ponds and photobioreactors. Bioresour. Technol. 101 (4), 1406–1413.

Kantzow, C., Mayer, A., Weuster-Botz, D., 2015. Continuous gas fermentation by *Acetobacterium woodii* in a submerged membrane reactor with full cell retention. J. Biotechnol. 212, 11–18.

Keller, M.W., Schut, G.J., Lipscomb, G.L., Menon, A.L., Iwuchukwu, I.J., Leuko, T.T., Thorgersen, M.P., Nixon, W.J., Hawkins, A.S., Kelly, R.M., et al., 2013. Exploiting microbial hyperthermophilicity to produce an industrial chemical, using hydrogen and carbon dioxide. Proc. Natl. Acad. Sci. USA 110 (15), 5840–5845.

Kim, S.W., Kim, P., Lee, H.S., Kim, J.H., 1996. High production of poly-beta-hydroxybutyrate (PHB) from *Methylobacterium organophilum* under potassium limitation. Biotechnol. Lett. 18 (1), 25–30.

Klamt, S., Mahadevan, R., Hädicke, O., 2017. When do two-stage processes outperform one-stage processes? Biotechnol. J. 13 (2), 1700539.

Knoop, H., Steuer, R., 2015. A computational analysis of stoichiometric constraints and trade-offs in cyanobacterial biofuel production. Front. Bioeng. Biotechnol. 3, 47.

Köhler, K.A.K., Rühl, J., Blank, L.M., Schmid, A., 2015. Integration of biocatalyst and process engineering for sustainable and efficient n-butanol production. Eng. Life Sci. 15 (1), 4–19.

Krainer, F.W., Dietzsch, C., Hajek, T., Herwig, C., Spadiut, O., Glieder, A., 2012. Recombinant protein expression in *Pichia pastoris* strains with an engineered methanol utilization pathway. Microb. Cell Fact. 11 (1), (22-22).

Lehtinen, T., Efimova, E., Tremblay, P.-L., Santala, S., Zhang, T., Santala, V., 2017. Production of long chain alkyl esters from carbon dioxide and electricity by a two-stage bacterial process. Bioresour. Technol. 243, 30–36.

Li, Y., Huang, B., Wu, H., Li, Z., Ye, Q., Zhang, Y.H.P., 2016. Production of succinate from acetate by metabolically engineered *Escherichia coli*. ACS Synth. Biol. 5 (11), 1299–1307.

Looser, V., Bruhlmann, B., Bumbak, F., Stenger, C., Costa, M., Camattari, A., Fotiadis, D., Kovar, K., 2015. Cultivation strategies to enhance productivity of *Pichia pastoris*: a review. Biotechnol. Adv. 33 (6), 1177–1193.

marketsandmarkets.com, 2016. Succinic Acid Market by Type (Bio-based, Petro-based), Application (Polyurethane, Resins, Coatings & Pigments, Pharmaceuticals, Plasticizers, Food & Beverage, PBS/PBST, Solvents & Lubricants, De-Icer Solutions, Personal Care, and Others), and by Region – Global Forecast to 2021. Market Report, Vol. CH 2917.

Mattozzi, M.d., Ziesack, M., Voges, M.J., Silver, P.A., Way, J.C., 2013. Expression of the sub-pathways of the *Chloroflexus aurantiacus* 3-hydroxypropionate carbon fixation bicycle in *E. coli*: toward horizontal transfer of autotrophic growth. Metab. Eng. 16, 130–139.

Mazière, A., Prinsen, P., Garcia, A., Luque, R., Len, C., 2017. A review of progress in (bio) catalytic routes from/to renewable succinic acid. Biofuel Bioprod. Bioref. 11, 908–931.

Michalowski, A., Siemann-Herzberg, M., Takors, R., 2017. *Escherichia coli* HGT: engineered for high glucose throughput even under slowly growing or resting conditions. Metab. Eng. 40, 93–103.

Mohan, S.V., Modestra, J.A., Amulya, K., Butti, S.K., Velvizhi, G., 2016. A circular bioeconomy with biobased products from CO_2 sequestration. Trends Biotechnol. 34 (6), 506–519.

Mourato, C., Martins, M., da Silva, S.M., Pereira, I.A.C., 2017. A continuous system for biocatalytic hydrogenation of CO_2 to formate. Bioresour. Technol. 235, 149–156.
Müller, J.E.N., Meyer, F., Litsanov, B., Kiefer, P., Potthoff, E., Heux, S., Quax, W.J., Wendisch, V.F., Brautaset, T., Portais, J.-C., et al., 2015. Engineering *Escherichia coli* for methanol conversion. Metab. Eng. 28, 190–201.
Nagarajan, H., Sahin, M., Nogales, J., Latif, H., Lovley, D.R., Ebrahim, A., Zengler, K., 2013. Characterizing acetogenic metabolism using a genome-scale metabolic reconstruction of *Clostridium ljungdahlii*. Microb. Cell Fact. 12 (1), (118-118).
Nogales, J., Gudmundsson, S., Knight, E.M., Palsson, B.O., Thiele, I., 2012. Detailing the optimality of photosynthesis in cyanobacteria through systems biology analysis. Proc. Natl. Acad. Sci. USA 109 (7), 2678–2683.
Nybo, S.E., Khan, N., Woolston, B.M., Curtis, W.R., 2015. Metabolic engineering in chemolithoautotrophic hosts for the production of fuels and chemicals. Metab. Eng. 30, 105–120.
Olah, G.A., 2005. Beyond oil and gas: the methanol economy. Angew. Chem. Int. Ed. 44 (18), 2636–2639.
Oliver, N.J., Rabinovitch-Deere, C.A., Carroll, A.L., Nozzi, N.E., Case, A.E., Atsumi, S., 2016. Cyanobacterial metabolic engineering for biofuel and chemical production. Curr. Opin. Chem. Biol. 35, 43–50.
Orgill, J.J., Atiyeh, H.K., Devarapalli, M., Phillips, J.R., Lewis, R.S., Huhnke, R.L., 2013. A comparison of mass transfer coefficients between trickle-bed, hollow fiber membrane and stirred tank reactors. Bioresour. Technol. 133, 340–346.
Orth, J.D., Conrad, T.M., Na, J., Lerman, J.A., Nam, H., Feist, A.M., Palsson, B.O., 2011. A comprehensive genome-scale reconstruction of *Escherichia coli* metabolism – 2011. Mol. Syst. Biol. 7 (1), (535-535).
Oswald, F., Dörsam, S., Veith, N., Zwick, M., Neumann, A., Ochsenreither, K., Syldatk, C., 2016. Sequential mixed cultures: from syngas to malic acid. Front. Microbiol. 7, 891.
Parikh, M.R., Greene, D.N., Woods, K.K., Matsumura, I., 2006. Directed evolution of RuBisCO hypermorphs through genetic selection in engineered *E. coli*. Protein Eng. Des. Sel. 19 (3), 113–119.
Pérez-Fortes, M., Schöneberger, J.C., Boulamanti, A., Tzimas, E., 2016. Methanol synthesis using captured CO_2 as raw material: techno-economic and environmental assessment. Appl. Energy 161, 718–732.
Pfeifenschneider, J., Brautaset, T., Wendisch, V.F., 2017. Methanol as carbon substrate in the bio-economy: metabolic engineering of aerobic methylotrophic bacteria for production of value-added chemicals. Biofuel Bioprod. Bioref. 11 (2), 719–731.
Phillips, J.R., Huhnke, R.L., Atiyeh, H.K., 2017. Syngas fermentation: a microbial conversion process of gaseous substrates to various products. Fermentation 3 (2), (28-28).
Pinazo, J.M., Domine, M.E., Parvulescu, V., Petru, F., 2015. Sustainability metrics for succinic acid production: a comparison between biomass-based and petrochemical routes. Catal. Today 239, 17–24.
Pontzen, F., Liebner, W., Gronemann, V., Rothaemel, M., Ahlers, B., 2011. CO_2-based methanol and DME-efficient technologies for industrial scale production. Catal. Today 171 (1), 242–250.
Qureshi, N., Annous, B.A., Ezeji, T.C., Karcher, P., Maddox, I.S., 2005. Biofilm reactors for industrial bioconversion processes: employing potential of enhanced reaction rates. Microb. Cell Fact. 4 (1), (24-24).
Rebnegger, C., Vos, T., Graf, A.B., Valli, M., Pronk, J.T., Daran-Lapujade, P., Mattanovich, D., 2016. *Pichia pastoris* exhibits high viability and a low maintenance energy requirement at near-zero specific growth rates. Appl. Environ. Microbiol. 82 (15), 4570–4583.
Santos, V.E.N., Ely, R.N., Szklo, A.S., Magrini, A., 2016. Chemicals, electricity and fuels from biorefineries processing Brazil's sugarcane bagasse: production recipes and minimum selling prices. Renew. Sustain. Energy Rev. 53, 1443–1458.
Savakis, P., Hellingwerf, K.J., 2015. Engineering cyanobacteria for direct biofuel production from CO_2. Curr. Opin. Biotechnol. 33, 8–14.
Schellenberger, J., Que, R., Fleming, R.M.T., Thiele, I., Orth, J.D., Feist, A.M., Zielinski, D.C., Bordbar, A., Lewis, N.E., Rahmanian, S., Kang, J., Hyduke, D.R., Palsson, B.Ø., 2011. Quantitative prediction of cellular metabolism with constraint-based models: the COBRA toolbox v2.0. Nat. Protoc. 6 (9), 1290–1307.
Schrader, J., Schilling, M., Holtmann, D., Sell, D., Villela Filho, M., Marx, A., Vorholt, J.A., 2009. Methanol-based industrial biotechnology: current status and future perspectives of methylotrophic bacteria. Trends Biotechnol. 27 (2), 107–115.
Schwander, T., Schada von Borzyskowski, L., Burgener, S., Cortina, N.a.S., Erb, T.J., 2016. A synthetic pathway for the fixation of carbon dioxide in vitro. Science 354 (6314), 900–904.
Shin, J., Song, Y., Jeong, Y., Cho, B.-K., 2016. Analysis of the core genome and pan-genome of autotrophic acetogenic bacteria. Front. Microbiol 7, 1531.
Straub, M., Demler, M., Weuster-Botz, D., Dürre, P., 2014. Selective enhancement of autotrophic acetate production with genetically modified *Acetobacterium woodii*. J. Biotechnol. 178, 67–72.
Tomas-Gamisans, M., Ferrer, P., Albiol, J., 2016. Integration and validation of the genome-scale metabolic models of *Pichia pastoris*: a comprehensive update of protein glycosylation pathways, lipid and energy metabolism. PLoS One 11 (1), e0148031.
Tomàs-Gamisans, M., Ferrer, P., Albiol, J., 2017. Fine-tuning the *P. pastoris* iMT1026 genome-scale metabolic model for improved prediction of growth on methanol or glycerol as sole carbon sources. Microb. Biotechnol. 11 (1), 224–237.
Valderrama-Gomez, M.A., Kreitmayer, D., Wolf, S., Marin-Sanguino, A., Kremling, A., 2016. Application of theoretical methods to increase succinate production in engineered strains. Bioprocess Biosyst. Eng. 40 (4), 479–497.
Van-Dal, É.S., Bouallou, C., 2013. Design and simulation of a methanol production plant from CO_2 hydrogenation. J. Clean. Prod. 57, 38–45.
van Maris, A.J.A., Geertman, J.M.A., Vermeulen, A., Groothuizen, M.K., Winkler, A.A., Piper, M.D.W., van Dijken, J.P., Pronk, J.T., 2004. Directed evolution of pyruvate decarboxylase-negative *Saccharomyces cerevisiae*, yielding a C_2-independent, glucose-tolerant, and pyruvate-hyperproducing yeast. Appl. Environ. Microbiol. 70 (1), 159–166.
Varma, A., Palsson, B.O., 1995. Parametric sensitivity of stoichiometric flux balance models applied to wild-type *Escherichia coli* metabolism. Biotechnol. Bioeng. 45 (1), 69–79.
Werpy, T.A., Holladay, J.E., White, J.F., 2004. Top Value Added Chemicals From Biomass: I. Results of Screening for Potential Candidates from Sugars and Synthesis Gas.
Whitaker, W.B., Jones, J.A., Bennett, R.K., Gonzalez, J.E., Vernacchio, V.R., Collins, S.M., Palmer, M.A., Schmidt, S., Antoniewicz, M.R., Koffas, M.A., et al., 2017. Engineering the biological conversion of methanol to specialty chemicals in *Escherichia coli*. Metab. Eng. 39, 49–59.
Young, J.D., Shastri, A.A., Stephanopoulos, G., Morgan, J.A., 2011. Mapping photoautotrophic metabolism with isotopically nonstationary ^{13}C flux analysis. Metab. Eng. 13, 656–665.
Zahrl, R.J., Peña, D.A., Mattanovich, D., Gasser, B., 2017. Systems biotechnology for protein production in *Pichia pastoris*. FEMS Yeast Res. 17 (7), fox068.
Zambanini, T., Kleineberg, W., Sarikaya, E., Buescher, J.M., Meurer, G., Wierckx, N., Blank, L.M., 2016. Enhanced malic acid production from glycerol with high-cell density *Ustilago trichophora* TZ1 cultivations. Biotechnol. Biofuels 9 (1), (135-135).
Zhang, D., Dechatiwongse, P., del Rio-Chanona, E.A., Maitland, G.C., Hellgardt, K., Vassiliadis, V.S., 2015. Dynamic modelling of high biomass density cultivation and biohydrogen production in different scales of flat plate photobioreactors. Biotechnol. Bioeng. 112 (12), 2429–2438.
Zhang, S., Bryant, D.A., 2011. The tricarboxylic acid cycle in cyanobacteria. Science 334 (6062), 1551–1553.
Zhao, J., Shimizu, K., 2003. Metabolic flux analysis of *Escherichia coli* K12 grown on ^{13}C-labeled acetate and glucose using GC-MS and powerful flux calculation method. J. Biotechnol. 101, 101–117.
Zhu, N., Xia, H., Yang, J., Zhao, X., Chen, T., 2014. Improved succinate production in *Corynebacterium glutamicum* by engineering glyoxylate pathway and succinate export system. Biotechnol. Lett. 36 (3), 553–560.
Zhuang, K.H., Herrgard, M., 2015. Multi-scale exploration of the technical, economic, and environmental dimensions of bio-based chemical production. Metab. Eng. 31, 1–12.